Pushover and Seismic Response of Foundations on Stiff Clay: Analysis with P-Delta Effects

Andriani I. Panagiotidou,[a] George Gazetas,[b] and Nikos Gerolymos[c]

Finite-element analyses are performed for the response to lateral monotonic, slow-cyclic, and seismic loading of rigid footings carrying tall slender structures and supported on stiff clay. The response involves mainly footing rotation under the action of overturning moments from the horizontal external force on—or the developing inertia at—the mass of the structure, as well as from the aggravating contribution of its weight (P-delta effect). Emphasis is given to the conditions for collapse of the soil-foundation-structure system. Two interconnected mechanisms of nonlinearity are considered: detachment from the soil with subsequent uplifting of the foundation (geometric nonlinearity) and formation of bearing-capacity failure surfaces (material inelasticity). The relation between monotonic behavior (static "pushover"), slow-cyclic behavior, and seismic response is explored parametrically. We show that with "light" structures uplifting is the dominant mechanism that may lead to collapse by dynamic instability (overturning), whereas "very heavy" structures mobilize soil failure mechanisms, leading to accumulation of settlement, residual rotation, and ultimately collapse. [DOI: 10.1193/1.4000084]

INTRODUCTION

An increasingly popular concept in structural earthquake engineering is the so-called pushover analysis. It refers to the nonlinear lateral force-displacement relationship of a particular structure subjected to monotonically increasing loading up to failure. The development (theoretical or experimental) of such pushover relationships has served as a key in simplified dynamic response analyses that estimate seismic deformation demands and their ultimate capacity.

In most cases, the development and use of such pushover relationships has either ignored the compliance of the supporting soil or, at most, has attached linear rotational springs to represent the global foundation-soil stiffness (Williamson 2003, Priestley 1993, 2003, Villaverde 2007). With the advent of performance-based design in engineering, the need has arisen to compute realistic pushover relationships for foundations. This calls for determining (in the terms of force-displacement or moment-rotation relations) the complete inelastic response of the foundation-soil system to progressively increasing lateral loads until collapse.

[a] Graduate Student, Massachusetts Institute of Technology, Cambridge, Massachusetts
[b] Professor, National Technical University, Athens, Greece
[c] Lecturer, National Technical University, Athens, Greece

Earthquake Spectra, Volume 28, No. 4, pages 1589–1618, November 2012; © 2012, Earthquake Engineering Research Institute

To this end, this paper investigates the lateral response of a shallow footing on stiff saturated clay supporting an elevated mass, which represents a comparatively tall, slender structure (Figure 1). This mass is being subjected to:

(i) Progressively increasing monotonic horizontal displacement until failure of the structure-foundation system;

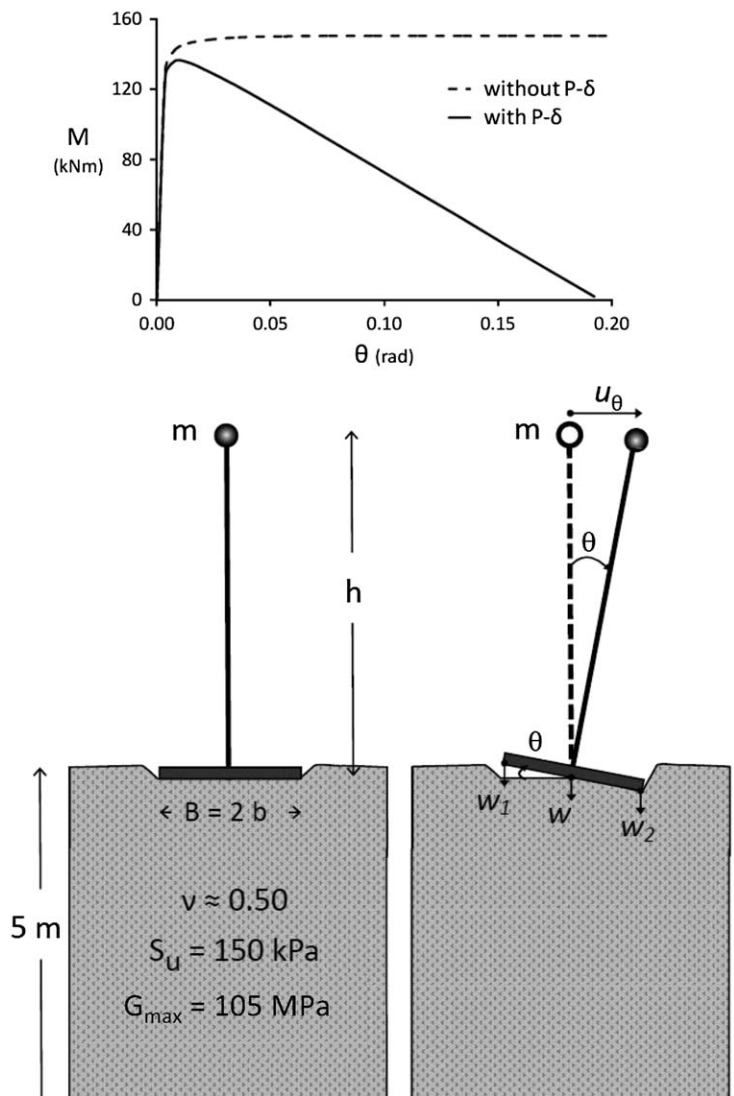

Figure 1. (a) Problem geometry and definition of response parameters; (b) overturning moment due to the horizontal force acting on the mass versus the (rigid-body) angle of rotation with and without $P - \delta$ effects.

(ii) Slow-cyclic horizontal displacement of progressively increasing amplitude (in both the ± direction), symmetrically around zero displacement; and
(iii) Seismic base excitations of different intensities and spectral characteristics.

In all cases, horizontal loading induces a large overturning moment and a moderate shear force. Initially, coupled rocking-swaying foundation oscillations (or just displacements for the static cases) take place under a linear soil response and complete contact at their interface. With increasing loads, the footing detaches and uplifts from the soil (geometric nearly-elastic nonlinearity), and soon afterward the soil response becomes nonlinear (material inelasticity). Eventually, a strong inelastic soil response is mobilized, culminating in the development of bearing-capacity failure mechanisms and accumulated settlement. All along, the rotation-induced lateral displacement ($u_\theta = \theta h$, where θ is the rotation of the foundation, and h is the height of the superstructure) of the superstructure mass (m) induces an additional (gravitational) aggravating moment (mgu_θ): the P–delta effect. At large displacements the role of this moment is crucial in driving the system to collapse.

The interplay between the nonlinear geometry (uplifting) and material inelasticity (soil failure) mechanisms, affected by the unavoidable P–delta effects, is governed primarily by the following factors (Figure 1):

- The vertical load ($N = mg$) in comparison with the ultimate vertical capacity (N_{ult}), expressed through the factor of safety ($FS_V = N_{ult}/N$)
- The slenderness ratio (h/b)
- The absolute size of the structure, measured, for instance, with the distance (R) between the center of gravity of the mass and the base edge
- The intensity, frequency content, duration, presence and sequence of strong pulses, and even details of the seismic excitation
- The fundamental period in rocking of the rigid structure on elastic base: $TR \approx 2\pi\sqrt{mh^2/K_R}$, where K_R is the elastic rotational stiffness of the foundation (given in Equation 4 below)

The emphasis of this paper is on the physics of the inelastic behavior of soil-foundation-structure systems and, especially on the conditions that would lead to collapse under the combined action of strong ground shaking and the destabilizing effect of the gravity load. It is considered that a particular loading (whether an external force on the mass or ground shaking) leads to collapse if the induced displacements and the gravity load reduce to zero the net restoring force in the system (Villaverde 2007). Note, however, one rare exception: Under seismic excitation, it is conceivable (even if highly improbable) that collapse might be avoided if loading were reversed at the very moment when the net restoring force reached zero. It is not in the scope of this paper to provide an extensive parametric study or to come up with definitive guidelines for the analysis and design of foundations (working at their limit, and beyond) Moreover, an experimental validation of some of our key findings is not provided here, but in a recently published paper (Drosos et al. 2012). However, some significant—even if only qualitative—vindication derives from the centrifuge work at the University of California at Davis (Rosebrook and Kutter 2001, Gajan et al. 2003 and 2005, Kutter et al. 2003).

BRIEF HISTORICAL NOTE

ROCKING ON A RIGID BASE

For over a century, since the pioneering work of Milne and Perry in 1881, the uplifting and overturning of rigid bodies has attracted the interest of many earthquake engineers and seismologists. Early analytical and experimental studies conducted mostly in Japan (and to some extent in the United States) have been motivated by the overturning of tombstones and monuments in large earthquakes. The early work of Kirkpatrick (1927) and Meek (1975) and the comprehensive historical review by Ishiyama (1998) were important contributions to the area of study.

Housner (1963) studied the rocking of a rigid block on a rigid base subjected to horizontal motion. Investigating the overturning potential, he unveiled a scale effect that makes large structures more stable against overturning than smaller ones with the same geometry and slenderness. He also realized the important role of the excitation frequency on the rocking response. Subsequently, several researchers have offered insights into the nature of the problem. Recently the phenomena have been further elucidated by Makris and Roussos (2000) and Shi et al. (1996), who subjected rigid blocks to trigonometric pulses and near-fault–type ground motions. It was shown that, under quasi-static conditions the (constant) critical acceleration (A_c) needed to uplift a block coincides with the acceleration required to topple it, and is equal to the inverse of the aspect ratio of the block (in units of g):

$$a_c \equiv \frac{A_c}{g} = \tan\,\theta_c = \frac{b}{h} \tag{1}$$

By contrast, it was shown that with seismic base motion, reaching and just exceeding A_c would rarely, if ever, cause overturning. This is attributed to the transient and oscillatory nature of seismic loading: Not only is the exceedance of A_c momentary, but also the reversal of acceleration "pulls the brakes" on the system, which decelerates before starting to rotate in the opposite direction. Apostolou et al. (2007) and Gerolymos et al. (2005) have shown that whether or not overturning occurs depends on the frequency content, the presence of long-duration pulses, and even the sequence of the pulses in the ground shaking. Ishiyama (1982), among others, studied swaying-rocking motion and established criteria for overturning versus sliding.

ROCKING ON ELASTIC SOIL

The response of a rigid block or system such as that in Figure 1 on viscoelastic soil differs from the response of the same structure or system on a rigid base because the compliance of the soil introduces additional degrees of freedom. A foundation on viscoelastic soil can undergo rotational motion, even before the initiation of uplifting (i.e., at amplitudes of rotation below a critical value). Once uplifting takes place, the (geometrically) nonlinear nature of the problem is evident, even under the assumption of a perfectly elastic soil. The latter plays the role of a "cushion," reducing the impact (and hence the structural foundation distress) after uplifting. The effect, however, on the overall stability of the system may range from beneficial to detrimental, depending on several other parameters.

Several analytical studies have investigated the effect of soil compliance on rocking with uplift. In most of these studies the underlying soil was represented by distributed tensionless linear spring-dashpot elements (Chopra and Yim 1984, Koh et al. 1986, Nakaki and Hart 1987, Houlsby et al. 2005). A few studies have modeled the soil as an elastic continuum (Apostolou et al. 2007). Shake table model experiments have also been performed using either a (relatively thin) soil layer or a (relatively thick) elastomeric pad as support (Huckelbridge and Clough 1978, Mergos and Kawashima 2005, Kawashima et al. 2007). These studies have emphasized the consequences of uplifting on the distress of superstructures such as buildings, bridge piers (Chen and Lai, 2003), and other massive structures (see also Paulay and Priestley 1992, Priestley et al. 1996). The concept of rocking isolation emerged from these studies, which showed that one of the important effects of uplifting is the elongation of the natural period of the system. In fact, a rocking block (even if rigid) at the moment of incipient instability (i.e., just at the initiation of toppling), exhibits a natural period that approaches infinity, regardless of how soft or stiff the soil is. This fact alone may explain the inherent robustness of these systems against gross instability, as ground motions hardly carry any energy at such large periods.

ROCKING ON INELASTIC SOIL

Inelastic action of at least a few soil elements under a footing is unavoidable even for a conservative static design. Under strong seismic shaking (causing uplifting) inelasticity would be expected to be widespread so that formation of continuous soil "failure" surfaces takes place. The possibility of such severe inelastic soil response and its effects on the structural response of a rigid block or system has been studied by several researchers. The methods that have been developed to model this hazard have been based on three broad categories of soil representation:

- Elastoplastic Winkler models (Bartlett 1976, Martin and Lam 2000, Allotey and El Naggar 2008, Harden et al. 2005 and 2006, Gerolymos and Gazetas 2006a, Harden and Hutchinson 2009)
- Inelastic continuum models, implemented by means of finite-element or finite difference algorithms (Wolf 1988, Paolucci 1997, Paolucci and Pecker 1997, Anastasopoulos et al. 2010, Gazetas et al 2007)
- Inelastic macroelements, that is, global force-displacement relations which, for each mode of vibration—vertical, horizontal, rocking—capture the material and geometric nonlinearities in the soil and at the interface (Allotey et al. 2003, Nova and Montrasio 1991, Gottardi et al. 1995, Pecker 1998, Cremer at al. 2002, Chatzigogos et al. 2009, Gajan and Kutter 2009a, Figini 2010). It is worth noting that in the elastic range, and without uplifting, the macroelement reduces to the familiar dynamic spring and dashpot (impedance) matrix (Veletsos and Wei 1971, Luco and Westman 1971, Kausel 1974, Roesset 1980, Gazetas 1991).

Moreover, the last decade has witnessed numerous experimental studies on centrifugal and 1 g shake tables, as well as on a large sandbox (Negro et al. 1998, Faccioli et al. 1998 and 2001, Rosebrook and Kutter 2001, Kutter et al. 2003, Gajan et al. 2003, Shirato et al. 2007, Shirato et al. 2008, Anastasopoulos et al. 2009). In view of the complexity of the problem, these studies have provided valuable data on the seismic response of sandy soil. (To our knowledge, only one test on clay has so far been reported in the literature on this subject: Gajan and Kutter 2008.)

Much of this work has been motivated by the National Earthquake Hazards Reduction Program (NEHRP) retrofit design guidelines (FEMA 2000), which specified the need for establishing the nonlinear lateral force-displacement ("pushover") failure characteristics of foundations, allowed the mobilization of bearing capacity mechanisms in the soil, and introduced a performance-based seismic design. Such design calls for assessing the magnitude of displacements and rotation of the foundation (both maximum and permanent values). It is worth noting, however, that the effects of yielding, rocking, and uplifting of rigid footings on the potential of a reduction in ductility demand of buildings had already been addressed by Taylor and Williams (1979).

The paper presents a numerical study for developing the pushover curves of a surface foundation carrying a relatively tall, slender structure (slenderness ratio: $h/b = 5$). Only undrained conditions are assumed to prevail in the soil, and the structure is considered absolutely rigid. The objectives of the paper are:

- To present pushover curves accounting for substantial P-delta effects and encompassing the complete range of foundation-soil behavior.
- To correlate static, monotonic, and cyclic loading with the seismic response, emphasizing the behavior at very large angles of rotation that may lead to collapse.
- To provide insight into the fundamental difference in response as a function of the static factor of safety (FS_V) against bearing capacity.

METHOD OF ANALYSIS

A series of two-dimensional finite-element analyses have been performed using ABAQUS software (Dassault Systèmes 2001). The soil is a saturated, stiff, homogeneous clay responding in an undrained fashion, with a shear strength of $S_u = 150$ kPa and a maximum shear modulus of $G_{max} = 105$ MPa. The bedrock is placed at a depth of 5 m below the foundation level. The mass element is located 5 m above the foundation level and is connected to the footing with rigid beam elements. The footing, with a width of $B = 2$ m, is also structurally absolutely rigid. The soil is modelled with continuum solid plane-strain four-noded bilinear elements forming a very refined mesh under the footing edges (Figure 2). Twenty

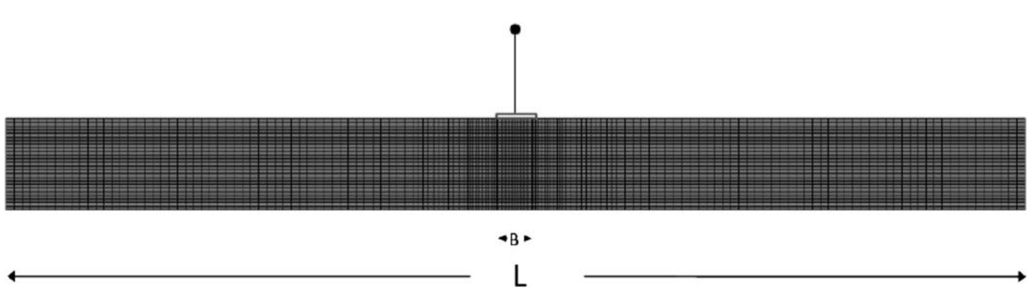

Figure 2. The finite-element discretization of the soil layer.

elements represent the ground surface under the footing. An advanced tensionless contact algorithm has been adopted to simulate the potential uplifting of the foundation. Gap elements allow the nodes to be in contact (gap closed) or separated (gap open). To achieve a reasonably stable time increment without jeopardizing the accuracy of the analysis, we modified the default hard contact pressure-overclosure relationship of ABAQUS with a suitable exponential relationship. A large coefficient of friction at the soil-footing interface (contact element) was deliberately chosen to prevent gross sliding of the footing on the soil surface.

The location and type of lateral boundaries were an important consideration in our dynamic modelling. Recall that whereas under monotonic and cyclic static loading these boundaries can be placed fairly close to the foundation (just outside the "pressure bulb") and they can be of any "elementary" type (from "free" to "fixed"), under dynamic loading, waves emanating from the footing-soil interface cannot propagate to infinity unless special transmitting boundaries are placed at suitably large distances. "Elementary" boundaries may cause spurious reflections, thereby contaminating the wave field below the foundation and reducing or even eliminating the radiation damping.

In this particular case, however, which refers to rocking-dominated vibrations of a slender structure, even "elementary" boundaries placed at a "reasonably large" distance from the foundation might suffice for the following three reasons:

(1) Static moment loading on the surface of a homogeneous halfspace induces normal vertical stresses, which decay very rapidly in both the horizontal and the vertical directions ("pressure bulb" of limited extent: less than one-half the width from the foundation edge, in either direction, Poulos and Davis 1974, Gazetas and Kavvadas 2009). Under low-frequency dynamic loading, waves emitted from symmetrically opposite points of the foundation contact surface, being out of phase, "interfere destructively," and thus substantially limit the radiation of wave energy (Veletsos and Wei 1971, Luco and Westman 1971, Kausel 1974, Gazetas 1987). Therefore, even in an (infinite) halfspace, boundaries placed at short distances from the loaded surface would hardly be "seen" by the waves emitted from the rocking foundation.

(2) The fundamental periods of the soil layer studied are less than 0.10 sec in shear and 0.05 sec in dilatation. These values, above which no radiation damping can develop (e.g., Kausel 1974), are far lower than both:

- The dominant period ranges of all exciting motions: $T_p \approx 0.5$ to 1.5 sec (as will be seen in the sequel to this paper)
- The period of rocking oscillations (T_R) of the slender system

Note that when large rotation after uplifting takes place, T_R increases substantially, above the full-contact elastic value of the rocking period and tends toward infinity at the critical angle of θ_c Therefore, radiation damping is negligible, and "elementary" boundaries placed at relatively short distances (a few widths) would suffice.

(3) In most of the cases analyzed, soil inelasticity is activated, mobilizing bearing capacity failure mechanisms. The presence of the associated localized failure surfaces (at shallow depths and small horizontal distances from the footing), has the effect of creating a softer zone inside the (stiffer) soil; this zone would reflect the incident waves, thus further reducing

the amount of wave energy transmitted ("leaking") into the surrounding soil (Borja et al. 1993 and 1994).

Indeed, Panagiotidou (2010) parametrically investigated the effect of the total width (L) of the FE (finite-element) discretized field. Even for a moderate level of shaking (for instance, the Takatori record from the 1995 Kobe, Japan earthquake downscaled to PGA = 0.20 g) an $L = 10B$ gives results that are hardly distinguishable from those for $L = 30B$. For stronger excitation levels, and consequently larger soil nonlinearities, radiation would be even more diminished and even smaller distances might be practically adequate. We have nevertheless adopted the $L = 10B$ distance in all studied cases to ensure that even under weak excitations (and hence, with an increasingly linear soil response, which is more conducive to radiation) no spurious reflections would contaminate the system response.

For the total stress analysis under undrained conditions, soil behavior is modeled through a nonlinear constitutive model (Gerolymos and Gazetas 2006b), which is a slight modification of a model incorporated in ABAQUS. It uses the von Mises failure criterion, with a yield stress (σ_y) that is related to the undrained shear strength (S_u) as:

$$\sigma_y = \sqrt{3}\, S_u \tag{2}$$

along with a nonlinear kinematic and isotropic hardening law and an associative plastic flow rule.

The model parameters are calibrated to fit the $G-y$ curves published in the literature. Figures 3a and 3b illustrate the validation of the kinematic hardening model (through simple shear finite-element analysis) against the $G-y$ curves by Ishibashi and Zhang (1993).

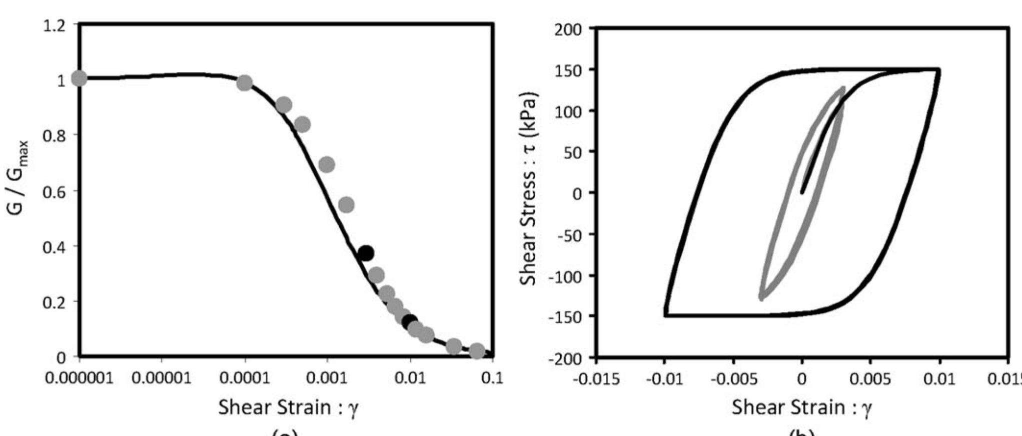

Figure 3. (a) Calibration of kinematic hardening model for soil (stiff clay, $S_u = 150$ kPa, $G_{max} = 700\, S_u$) against published $G-\gamma$ ($PI = 30$, $\sigma_v' = 200$ kPa) curves (Ishibashi and Zhang 1993); (b) s stress-strain loops corresponding to the designated (black-colored) points in (a).

The performance of the above constitutive law, along with the numerical model, were successfully tested (errors of less than 5%) by comparing the computed static vertical ultimate bearing capacity (N_{ult}) failure against the classical analytical solution by Prandtl:

$$N_{ult} = (\pi + 2)\, S_u\, B \tag{3}$$

For the considered undrained shear strength $S_u = 150$ kPa, Equation 3 gives $N_{ult} \approx 1542$ kN.

Furthermore, the initial practically elastic rotational stiffness of the footing (before the initiation of uplift) was consistent with the analytical solution (e.g., Dobry and Gazetas 1986),

$$K_R \approx \frac{\pi\, G\, B^2}{8\,(1-\nu)} \left(1 + \frac{1}{10}\frac{B}{H}\right) \tag{4}$$

in which G and ν are the shear modulus and Poisson's ratio of the soil, respectively, B is the footing width, and H is the depth to bedrock. We are confident in the employed methodology for monotonic loading conditions. However, the employed associative flow rule would hardly provide a perfect representation of the cyclic response. We thus: (i) consider our results approximate, (ii) insist on experimental corroboration (qualitative, at least), and (iii) place our emphasis on the trends rather than on the numbers resulting from the analyses.

RESULTS: STATIC PUSHOVER ANALYSIS

For a static pushover analysis a horizontal displacement is applied to the mass of the superstructure. A set of results portrayed in Figure 4 show the nature of the response. The moment-rotation diagrams for three static vertical safety factors ($FS_V = N_{ult}/N = 5,\ 2,$ and 1.25) are portrayed in this figure, along with the ultimate M-N interaction diagram (in the form M_{ult}–N/N_{ult}). As expected, the largest value for moment capacity is reached for a static safety factor of about $FS_V \approx 2$ (Georgiadis and Butterfield 1988, Salençon and Pecker 1995, Allotey and Naggar 2003, Apostolou and Gazetas 2005, Chatzigogos et al. 2009, Gajan and Kutter 2008). The choice of the other factors of safety is somewhat arbitrary, aiming to achieve two different behaviors, that of a heavily loaded foundation ($FS_V = 1.25$, which is typical of many monumental structures such as, for instance, the Tower of Pisa) where the failure mode is related to the bearing capacity of the foundation and that of a typical conservatively designed (moderately to lightly loaded) foundation with $FS_V = 5$, for which uplift is the predominant failure mechanism.

In Figure 4, for each of the three cases (1, 2, and 3) corresponding to the values of $FS_V = 5$, 2, and 1.25, respectively, we display three snapshots of the deformed system along with the contours of plastic deformation in the soil. Specifically, Figures 1a, 2a, and 3a present the initial (static) state under vertical loading only, $N = 308$, 771, and 1,234 kN. Figures 1b, 2b, and 3b show the states at the peak moment, $M_{ult} = 238$, 354, and 232 kNm, respectively. And Figures 1c, 2c, and 3c show the states at imminent collapse.

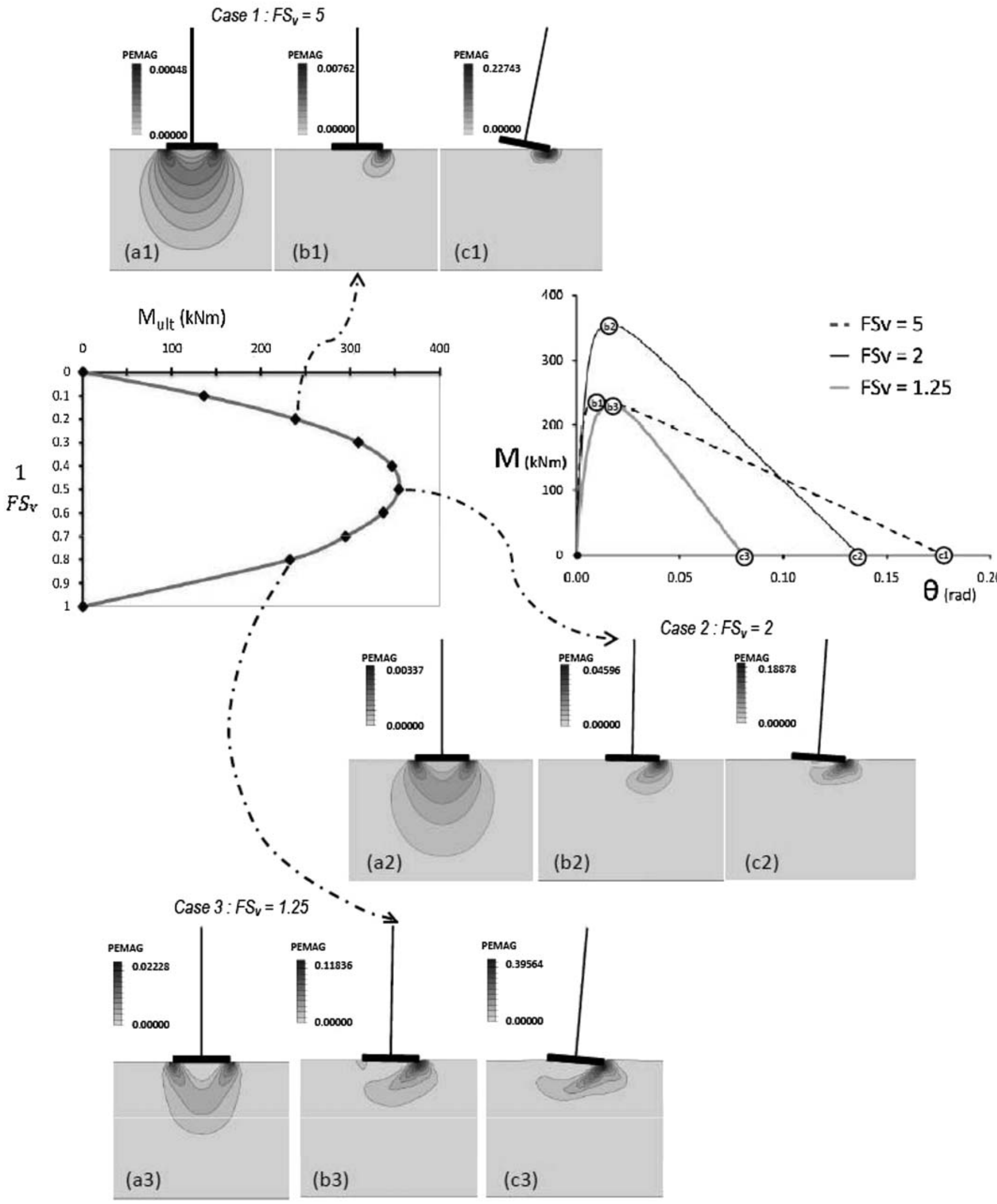

Figure 4. $M - N$ interaction diagram, relating the statically-applied ultimate (overturning) moment to the $1/FS_V = N/N_{ult}$, that is, to the vertical load N (= mg) normalized by the static vertical capacity $N_{ult} = (\pi + 2)S_uB$, where S_u is the undrained shear strength of soil and B is the width of footing. For three points in the diagram (corresponding to $FS_V = 5, 2,$ and 1.25), we plot the complete $M - \theta$ response curves showing the strong post-peak decline due to the additional moment from gravity (P – δ effect). Also displayed for each FS_V are three snapshots of the deforming system along with the contours of plastic shear deformations in the soil. a1, a2, and a3 show the initial static state; b1, b2, and b3 occur at the instant of the maximum (ultimate) overturning moment (M_{ult}); and c1, c2, and c3 are the states at the instant of imminent collapse.

The interaction curve in Figure 3 can be also approximated analytically (without consideration of the P-delta effects) as a function of the static factor of safety (FS_V) according to the following relationship (Apostolou and Gazetas 2005):

$$M_{ult} = \frac{1}{2\,FS_V}\left(1 - \frac{1}{FS_V}\right)N_{ult}\,B \tag{5}$$

Note that the maximum moment is reached soon after the threshold of uplifting has been exceeded, at a relatively small rotation. As the static vertical safety factor (FS_V) diminishes, the rotation angle (θ_c) at the state of imminent collapse ("critical" rotation) also decreases. Indeed, for rocking on compliant soil, θ_c is always lower than it is on a rigid base (given with Equation 1).

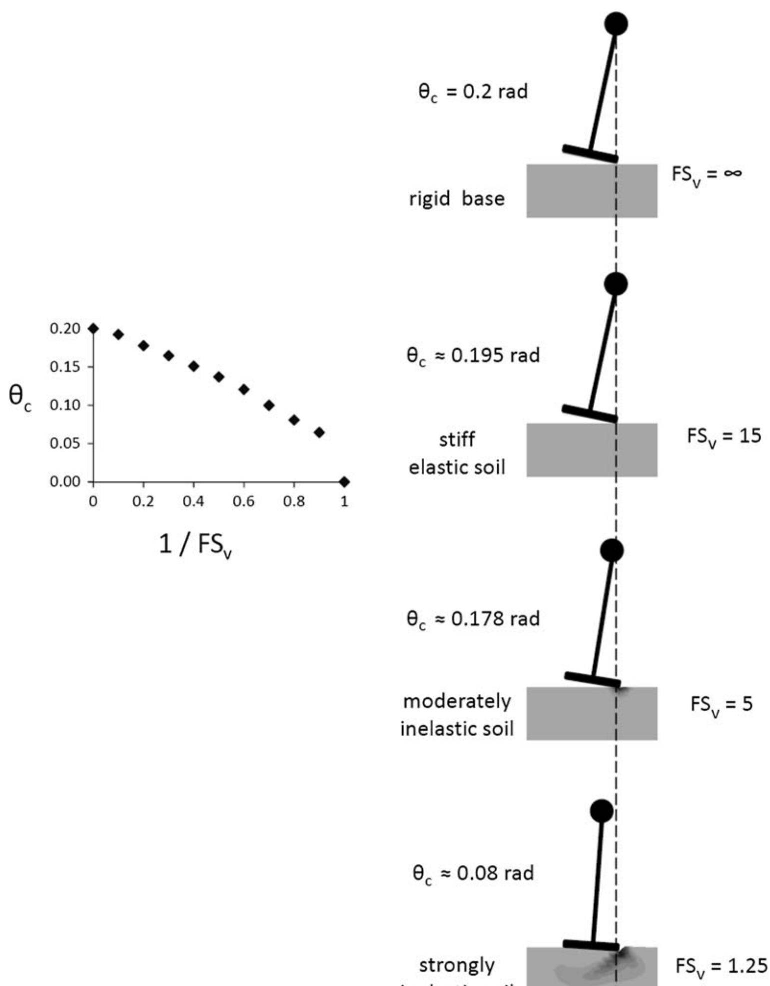

Figure 5. Illustration of the angle of imminent collapse as a function of the static factor of safety (FS_V).

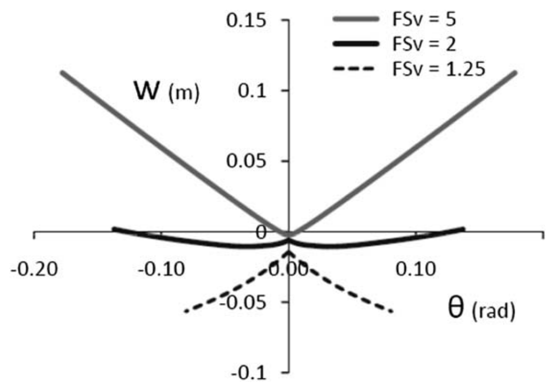

Figure 6. Monotonic settlement (−) or uplift (+), w, versus angle of rotation (θ) for three FS_V values.

As illustrated in Figure 5, for stiff elastic soil (or with a very large static vertical safety factor) θ_c is imperceptibly smaller than that given by Equation 1, because the soil deforms slightly only below the (right) edge of the footing and therefore only insignificantly alters the geometry of the system at the point of overturning. As the soil becomes softer, soil inelasticity starts playing a role in further reducing θ_c. However, such a reduction is small as long as the factor of safety (FS_V) remains high (say, in excess of 3). Such behavior changes drastically with a very small FS_V: then the soil responds in strongly inelastic fashion, until a bearing-capacity failure mechanism develops, replacing uplifting as the prevailing mechanism leading to collapse.

In conclusion, for slightly inelastic soil (which can be due to either a high undrained shear strength or to light loading) θ_c approaches the value given by Equation 1 for a block on rigid base. For strongly inelastic soil (either due to a small undrained shear strength or to heavy loading) θ_c decreases, tending obviously to zero for an $FS_V = 1$.

Also of interest are the corresponding monotonic settlement-rotation ($w - \theta$) curves given in Figure 6. Notice that with high FS_V (e.g., $FS_V = 5$) the system undergoes monotonically increasing uplift with an increasing angle of rotation, while with very low FS_V (e.g., $FS_V = 1.25$) it suffers monotonically increasing downward deformation and settlement. In the intermediate case, when $FS_V = 2$, there is initially a slight increase in settlement at small θ, which gives way to slight uplifting at larger θ.

RESULTS: CYCLIC PUSHOVER ANALYSIS

Slow cyclic results are shown for the three systems having high, medium, and low factors of safety ($FS_V = 5$, 2, and 1.25, respectively). The displacement imposed on the mass center increased gradually; the last cycle persisted until collapse. The choice of the values of the above displacements was made in view of the monotonic pushover results. As can be seen in the moment-rotation diagrams, the loops of the cyclic analyses for safety factors greater than 2 are well enveloped by the monotonic pushover curves (in Figure 7a, in fact, the static and maximum cyclic curves are indistinguishable). This can be explained by the fact that the plastic deformations that take place under the edges of the foundation during the

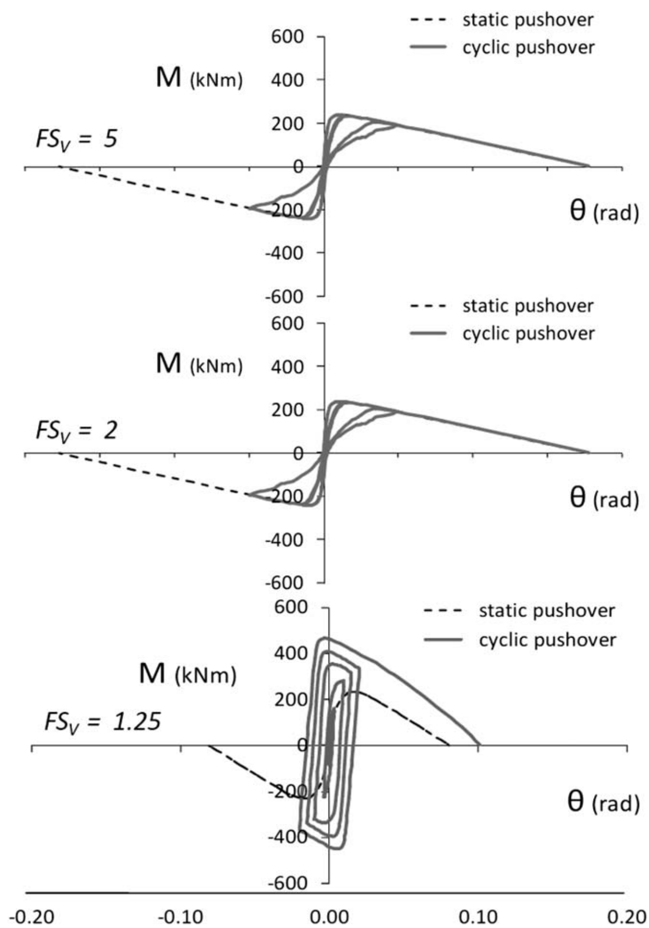

Figure 7. Superimposed monotonic and cyclic pushover $M - \theta$ curves for three FS_V values.

deformation-controlled cyclic loading are too small to affect to any appreciable degree of response of the system when the deformation alters direction (Figure 8). As a consequence, the residual rotation vanishes after a complete set of cycles—an important (and desirable) characteristic. The system largely rebounds, helped by the restoring role of the weight. A key factor of this response is the small soil deformations thanks to the light load of the foundation. Effectively, the soil is nearly undeformable at such large FS_V values.

The cyclic response for the $FS_V = 2$ system is also essentially enveloped by the monotonic pushover curves. However, the hysteresis loops are now wider and residual rotation appears upon a full cycle of loading, as inelastic deformations in the soil are now substantial.

The above behavior is qualitatively similar to the results of centrifuge experiments conducted at the University of California at Davis (e.g., Kutter et al. 2003, Gajan et al. 2005) and large-scale tests conducted at the European Joint Research Centre, in Ispra (Negro et al. 2000, Faccioli et al. 1998).

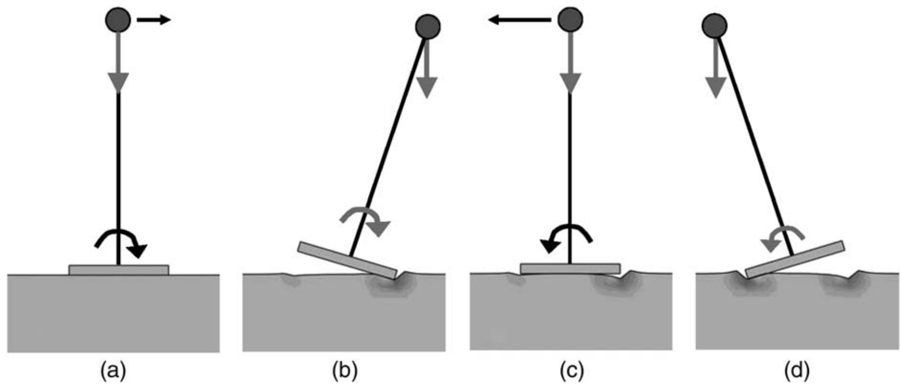

Figure 8. Snapshots from the FE analysis illustrating a loading (a–b), unloading (b–c), and reloading (c–d) half-cycle of a complete cycle of imposed rotation on a lightly loaded foundation ($FS_V > 5$), sketching the forces on the mass, the resulting overturning moments onto the foundation, and the zones of mobilized soil strength. Yielding of the soil is very limited, alternating under the edges of the footing. Note color agreement (black vs. gray) between force and moment.

However, the response of the heavily loaded system ($FS_V = 1.25$) is markedly different. The $M-\theta$ loops are no longer enveloped by the monotonic pushover curves (Figure 7c). It seems that the moment capacity of the system depends on the rotation of the previous step, and as the rotation increases, the difference between the two curves (cyclic versus monotonic) increases. This striking behavior could be attributed to the large soil deformation and the changing role of P-delta effects, as illustrated below.

We attempt to explain this behavior by recourse to the sketches in Figure 9, for a foundation with an $FS_V = 1.25$ (clearly an extreme, but not impossible case: examples can be found in historic monumental structures, such as the Tower of Pisa). First, notice that, footing and soil remains practically in full contact even at comparatively large rotation angles. The displacement-controlled cyclic loading at the mass center transmits a moment on the footing, say in the clockwise direction (Figure 9a), which beyond a certain amplitude mobilizes bearing capacity-type failure mechanisms. Such mechanisms involve:

- A shallow rotational failure under the pushed-in right edge of the footing. The well-defined sliding surface, passing through the zone of excessive shearing deformation (as shown by the dark line in Figure 9b), extends a small distance beyond the footing; the soil moves outward, to the right.
- A deeper rotational movement under the upward-moving left side of the foundation, with a diffuse failure zone (rather than a single surface) extending beyond the edge of the footing, and producing a significant bulge of the soil-footing interface, as the soil moves leftward and upward (Figure 9b).

As a result, when the loading direction is reversed, the foundation, first, has to surmount the “hill” (bulging) created in the preceding cycle (highlighted in Figure 9c). Second, and perhaps more significantly, the imposed external moment is no longer undermined by the P–delta effects; it is now enhanced (not reduced) by the moment of the weight of the

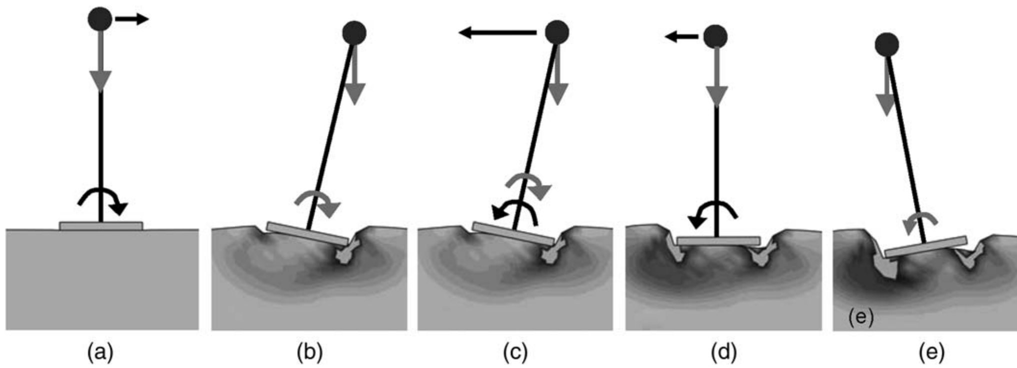

Figure 9. Snapshots from the FE analysis offering a plausible explanation (not quite a proof yet) of the overstrength observed during the reloading cycle of a heavily loaded foundation ($FS_V = 1.25$). The five stages of a loading cycle are: (a) imposition of a (rotation-controlled) horizontal force to the right, (b) the system approaches its largest rotation and the weight produces an overturning moment balanced by the reactions of the pushed-in soil, (c) the system, forced to the left, develops its maximum resisting moment before crossing the vertical axis, when the weight produces a beneficial counter-moment, (d) and (e) the system passes through the vertical axis and eventually reaches the largest rotation in the other direction (without any applied moment).

structure, which is acting in the opposite (i.e., rightward) direction (Figure 9c). Thus a much larger imposed external moment is needed for equilibrium with a given rotation, hence the apparent "overstrength." Thereafter the process is repeated. Upon exceeding the point of zero rotation (Figure 9d), the weight starts acting again in the counterclockwise direction, thus once more aggravating the tendency for overturning (Figure 9e); two new failure mechanisms are created in the soil and the cycle is repeated.

A first experimental piece of evidence for the development of overstrength has indeed been derived in small-scale 1 g shake table tests on sand, to be presented by Drosos et al. (2012, submitted companion paper).

To further elucidate the source of the observed overstrength in the system response, Figures 10a and 10b show the shear stress-strain loops at distance (x, z) = (0.5 m, 0.5 m) from the foundation center, for a moderately-to-lightly loaded ($FS_V = 5$) and a heavily loaded ($FS_V = 2$) footing. The mass of the superstructure is subjected to a displacement-controlled time history of four cycles and constant amplitude (δ_0). The latter is such that the ratio of the maximum developed overturning moment at the foundation center to the ultimate moment capacity of the foundation is the same for the two structures, equal to 3.2 (0.25 cm for the moderately-to-lightly loaded foundation and 0.16 cm for the heavily loaded one).

It is interesting to observe in Figure 10 that the ultimate shear strength does not exceed the undrained shear strength (S_u = 150 kPa). This implies that material hardening due to cyclic loading is not reproduced by the utilized constitutive model, providing additional evidence that P-delta effects could be the only possible source of the observed overstrength in the system response.

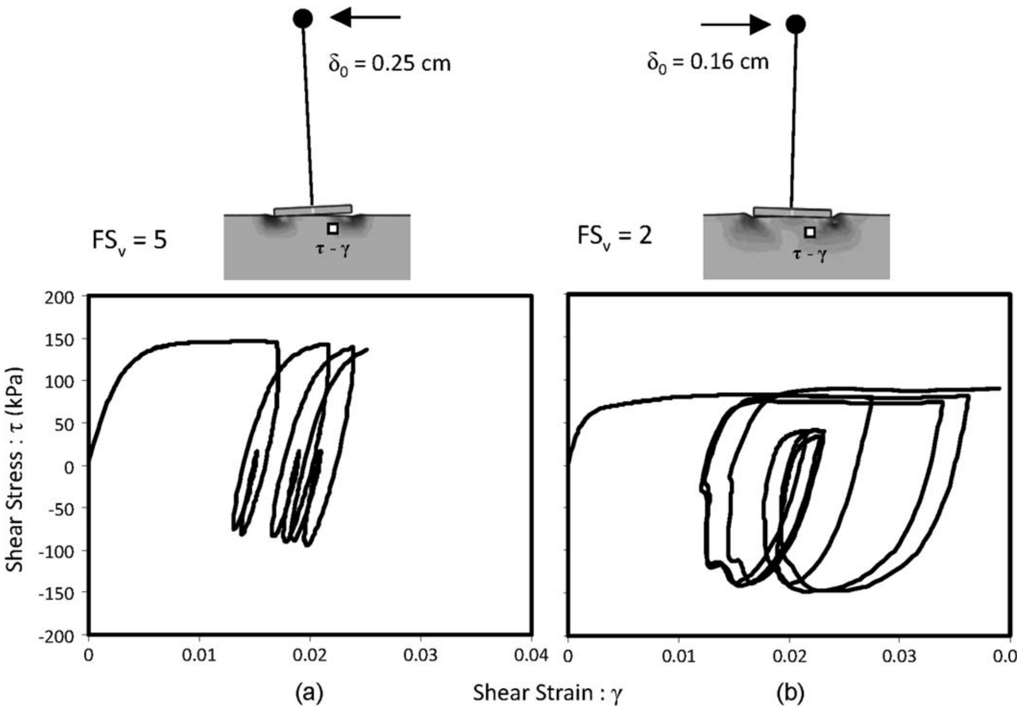

Figure 10. (a) and (b) Shear stress-strain loops calculated at distance (x, z) = (0.5 m, 0.5 m) from the foundation center, for the moderately-to-lightly loaded $(FS_V = 5)$ and the heavily loaded $(FS_V = 2)$ foundation, respectively. The mass of the superstructure is subjected to a displacement-controlled time history of four cycles and a constant amplitude (δ_0). The latter is such that the ratio of the maximum developed overturning moment at the foundation center to the ultimate moment capacity of the foundation is the same for the two structures, equal to 3.2.

RESULTS: SEISMIC ANALYSIS

LATERAL RESPONSE

The records of Takatori (1995 Kobe earthquake), Kalamata–1 (1986 Kalamata earthquake), and Lefkada (2003 Lefkada earthquake) are used as rock excitation. Since the fundamental (elastic) period of the soil stratum in shear is merely 0.08 sec, neither soil amplification of upward propagating waves nor any appreciable radiation damping from outward spreading foundation-produced waves take place with the above base motions, the dominant periods of which are in the range of $T_p \approx 0.5$ to 1.5 sec. Takatori was selected as one of the most severe ground motions ever recorded, especially for flexible and inelastic systems, owing to its richness in high-period components. The two other accelerograms were selected to study the effect of the frequency content of the excitation. To study the response as a function of excitation intensity we have scaled these motions to PGA values ranging from 0.1 to 0.9 g. The results for seismic analyses are shown in Figures 11 through 18.

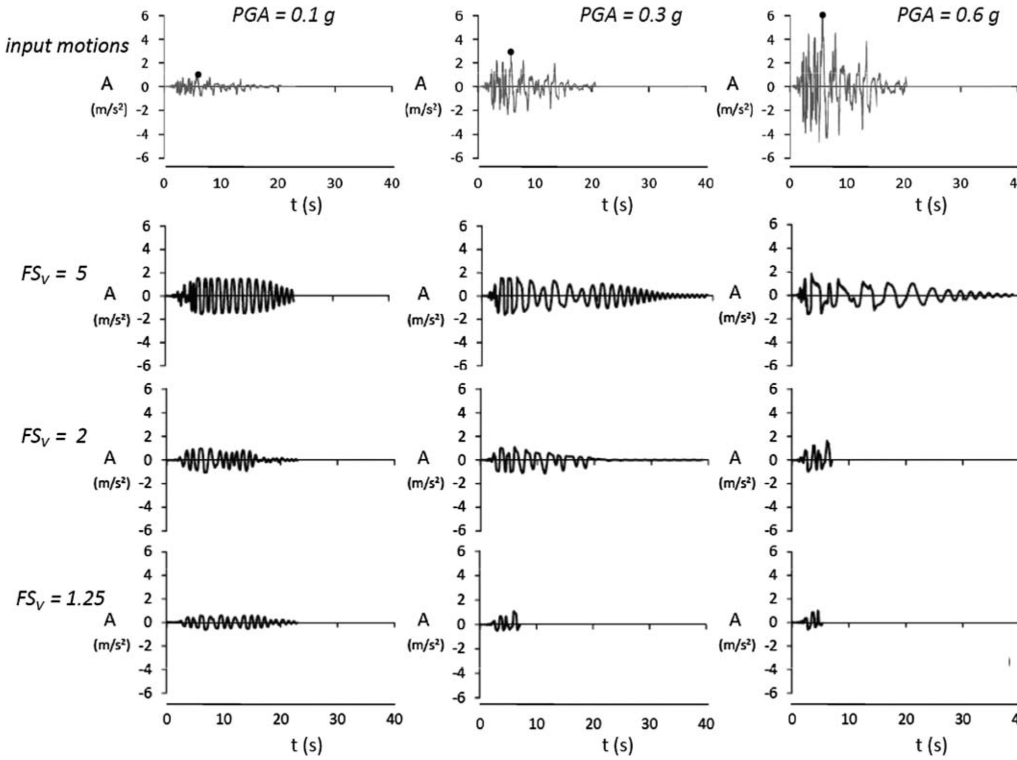

Figure 11. Acceleration time histories of the mass for three different FS_V factors, in response to three down-scaled Takatori records (PGA = 0.1 g, 0.2 g, and 0.6 g).

For three static vertical safety factors ($FS_V = 5$, 2, 1.25), Figure 11 displays the computed time histories of acceleration at the mass of the oscillator. The input motions (shown in the top row) are from the Takatori record downscaled to 0.1, 0.3, and 0.6 g. Observe that for a given motion intensity the developing acceleration is profoundly dependent on the static safety factor (FS_V) of the system: The higher FS_V the higher the acceleration. On the other hand, the dominant period of oscillation depends both on FS_V and PGA.

In Figure 12, the moment-rotation diagrams are shown for the same six cases as in Figure 11. Naturally, for a given FS_V, the larger PGA brings about stronger inelastic action in the soil-foundation system, thereby maximum and residual deformations increase. The moment-rotation diagrams confirm the behavior already noted with cyclic loading. For large FS_V (e.g., 5) the $M-\theta$ curves are confined within the monotonic static pushover curve, which acts as an envelope. And the residual rotation is negligible, as the unloading and reloading curve invariably pass through $\theta = 0$. On the other hand, for very small FS_V (e.g., 1.25) the loops that are produced during seismic response go substantially above the bounds of the static pushover curves. Only the first half cycle is indeed enveloped by the monotonic curve. Thereafter, as the soil exhibits large deformations due to its high compliance under the heavy vertical load, moment-bearing capacity failure mechanisms

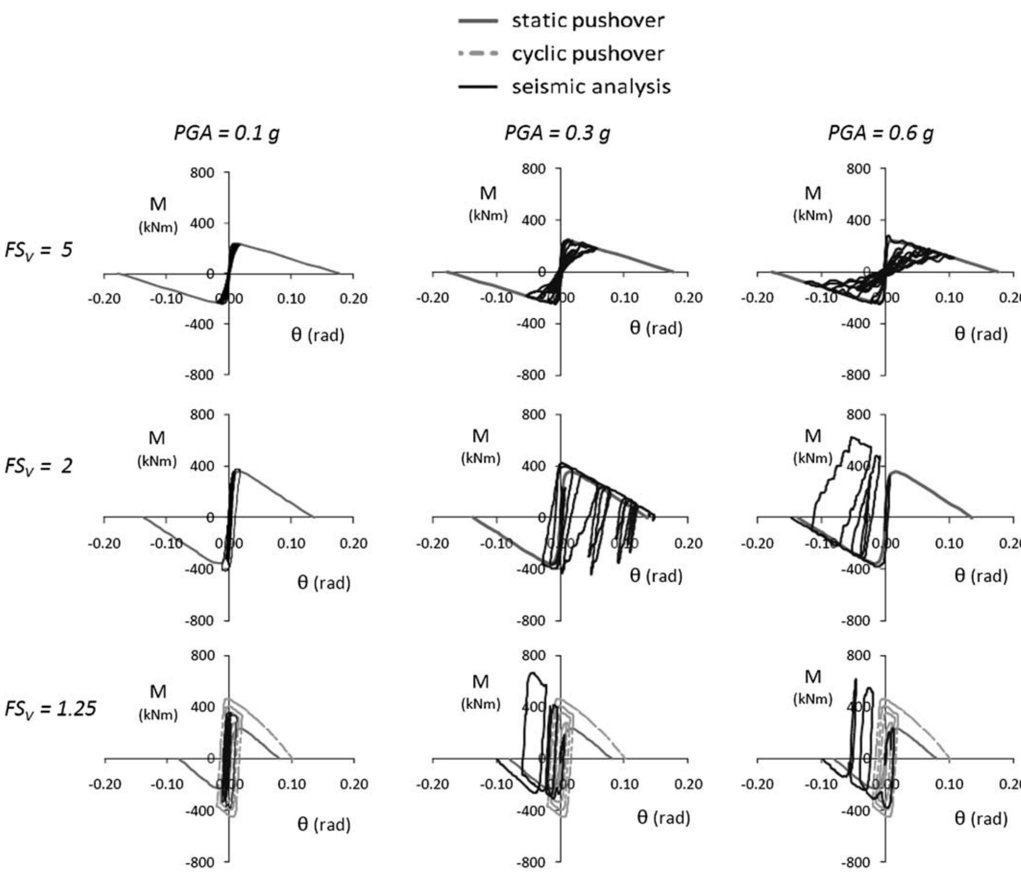

Figure 12. The seismic $M-\theta$ loops for each of the nine cases in Figure 9 superimposed on the monotonic pushover curves (for $FS_V = 1.25$, the cyclic loops are also superimposed).

develop and affect the behavior of the system, as was previously explained in connection with cyclic loading in Figure 9. The result: highly asymmetric behavior. Notice that on the plots for $FS_V = 1.25$ (the last row of plots in of Figure 12) we have superimposed with dotted lines the cyclic $M-\theta$ curves from Figure 7c, just to confirm the similarity in the observed overstrength.

To further elucidate the appearance and surprising consequences of this remarkable (cyclic) overstrength, time histories of mass acceleration, footing rotation, and the respective $M-\theta$ curve, are presented in Figure 13 for the case of $FS_V = 1.25$ and Takatori with PGA = 0.6 g. The motion starts at Point 1. The first large deformation takes place to the right (Point 2). Then the acceleration changes direction and, soon after, the system starts rotating in the opposite direction. After passing from the point of zero rotation (Point 3), the inertial force still acts to the left, leading the footing a little closer to overturning (Point 4). The acceleration changes direction once more, and therefore the oscillator soon tends to rotate clockwise; but it is still tilting to the left ($\theta < 0$). Thus, now, the foundation has to surmount: (a) the

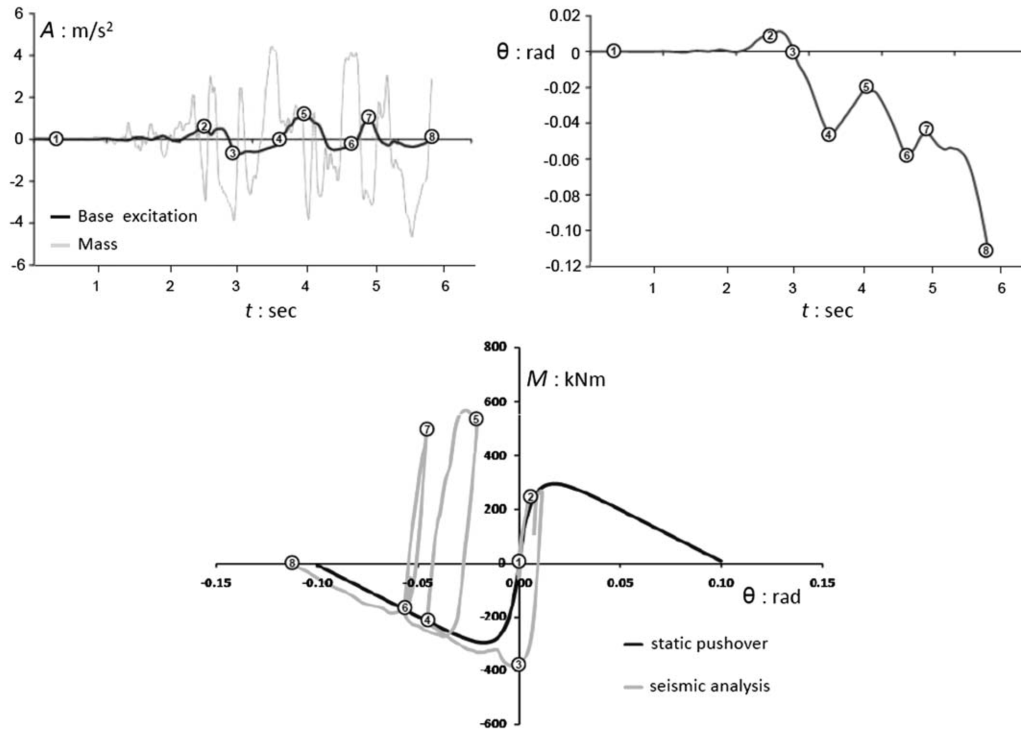

Figure 13. Tracing the “path to collapse”: $FS_V = 1.25$, Takatori, 0.60 g excitation. The substantial de-amplification of acceleration due to the easily forming “plastic hinge” under this heavily loaded foundation is not enough to save it. Despite the overstrength (or, in fact, paradoxically because of it) the system at Point 4 cannot overcome its one-sided rotation, and recovers only to a small extent (Point 5), so that the additional long-period pulses drive it to failure.

excessive bulge of the ground under the upward moving part of the foundation created in the preceding cycle and (b) the counter moment of the weight. This can only be achieved if the applied load (and hence moment) is enhanced. Consequently, the system displays overstrength (Point 5), but still it does not enjoy a change in the direction of tilting (Point 5 still has $\theta < 0$). Therefore it is easier (because of the overstrength) to move the system further down to the left (Point 6) when the next acceleration pulse arrives. This process is repeated every time the acceleration changes first to the right and then to the left (Points 7 and, finally, 8) when the system eventually (and almost inevitably) overturns. Surprisingly, therefore, the overstrength plays a detrimental, not a beneficial, role in this particular case. However, the predictability of such a phenomenon is a formidable task, in view of its sensitivity to the unloading-reloading characteristics.

In conclusion, for the majority of engineered new structures (which would prudently have safety factors greater than 2) the monotonic pushover curves are representative of the moment capacity of the system, even under seismic loading. For structures that have safety factors well below 2 (such as many monumental structures built centuries ago with no knowledge of the subsoil), the maximum moment they can sustain cannot be determined a priori as this is a function of the preceding rotation, and, naturally, a sensitive function of the amplitude and duration of the seismic pulse at that moment. The cyclic pushover curves are an approximate representation of the behavior of the system. Undoubtedly, more research is needed to further illuminate this behavior.

Finally, it is worth mentioning that when the system with $FS_V = 2$ and PGA = 0.3 g (Figure 12) reaches the point of precarious equilibrium and the rotation is almost equal with its critical value, the moment capacity of the structure vanishes but the structure, rather fortuitously, does not topple!

SETTLEMENT AND UPLIFT

For the sake of brevity, only two extreme FS_V cases (5 and 1.25) are presented in Figure 14 for two rather extreme PGA values (0.1 g and 0.6 g) in the form of $w - \theta$ relationships. The dramatic disparity in the behavior of the two systems is apparent. For $FS_V = 5$ the seismic $w - \theta$ curves follow more or less the pair of its monotonic curves, which, as already discussed, are characterized by severe uplifting with only minor (if any) additional settlement. For $FS_V = 1.25$ the $w - \theta$ curves are not bound by the respective monotonic curve, showing an accumulating settlement and, for PGA = 0.6 g, accumulating permanent tilt, implying collapse (as already discussed).

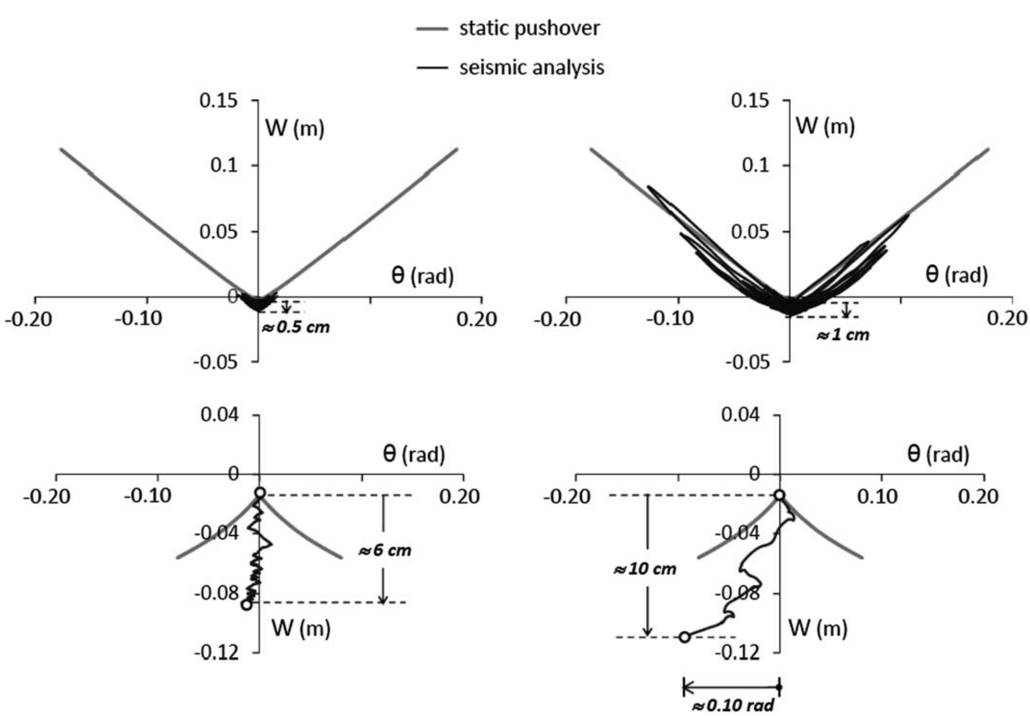

Figure 14. Settlement (−) or uplift (+), w, versus rotation angle θ, for two FS_V factors (5 top row, 2 bottom row), and two down-scaled Takatori motions (PGA = 0.2 g, left column; PGA = 0.6 g, right column).

An important difference is mentioned between the response of a moderately-to-lightly loaded $(FS_V \geq 5)$ foundation on clay under undrained conditions, as studied theoretically here, and the same lightly loaded foundation on dry sand, as investigated in shake table experiments (under 1 g or centrifugal conditions). Whereas on (incompressible) clay the foundation center undergoes mainly uplifting cycles and ends up with little, if any, additional settlement (beyond the static one), on (compressible) dry sand the repeated cycles of impact tend to produce an accumulation of settlement, despite the temporary uplift of the foundation edges (see experimental evidence in Gajan and Kutter 2009a and 2009b for deeper insight and additional results).

Figure 15 further elucidates this behavior by plotting the ratio:

$$\lambda = \lambda(t) = \frac{\beta(t)}{B} \tag{6}$$

of the width of the effective contact $[\beta = \beta(t)]$ divided by the (total) width (B) of the footing. (Note that the discontinuous form of the $\lambda(t)$ plots is an undesirable but unavoidable consequence of the discretization of the contact surface.) The meaning of these curves is rather obvious. Notice in particular that the $FS_V = 1.25$ system attains with both PGAs almost full contact $(\lambda(t) > 0.75)$, although with PGA = 0.60 g bearing capacity failure under the gravity-driven additional overturning moment (mgu_θ) leads eventually to $\lambda = 0$, or collapse by overturning.

Nevertheless, it is remarkable that several systems with high FS_V can avoid overturning despite reaching values of λ as low as 0.125, thanks to the cyclic and kinematic nature of seismic loading.

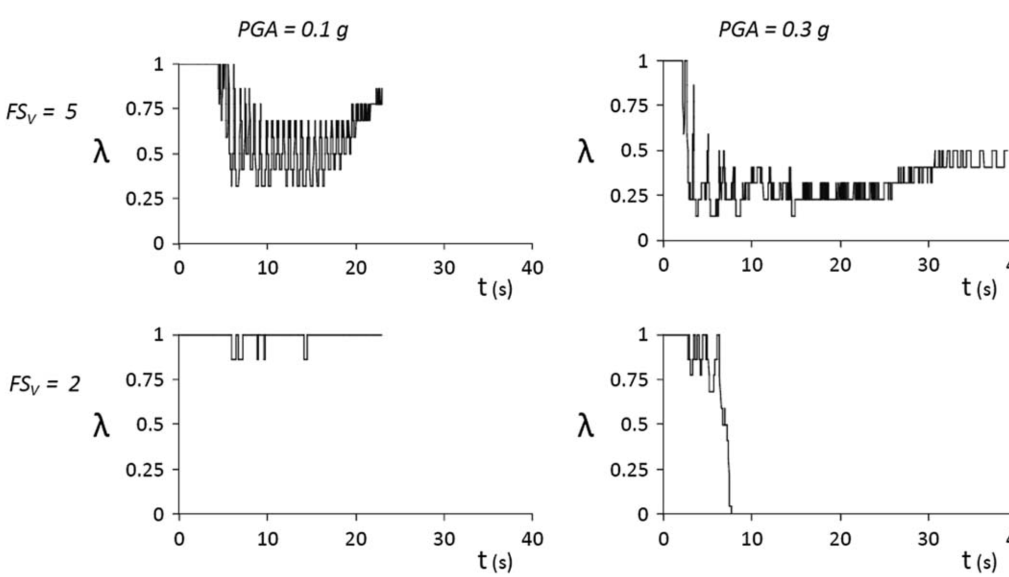

Figure 15. Time histories of the fraction of the width of the footing that is in contact with the soil, for the four cases examined in Figure 12.

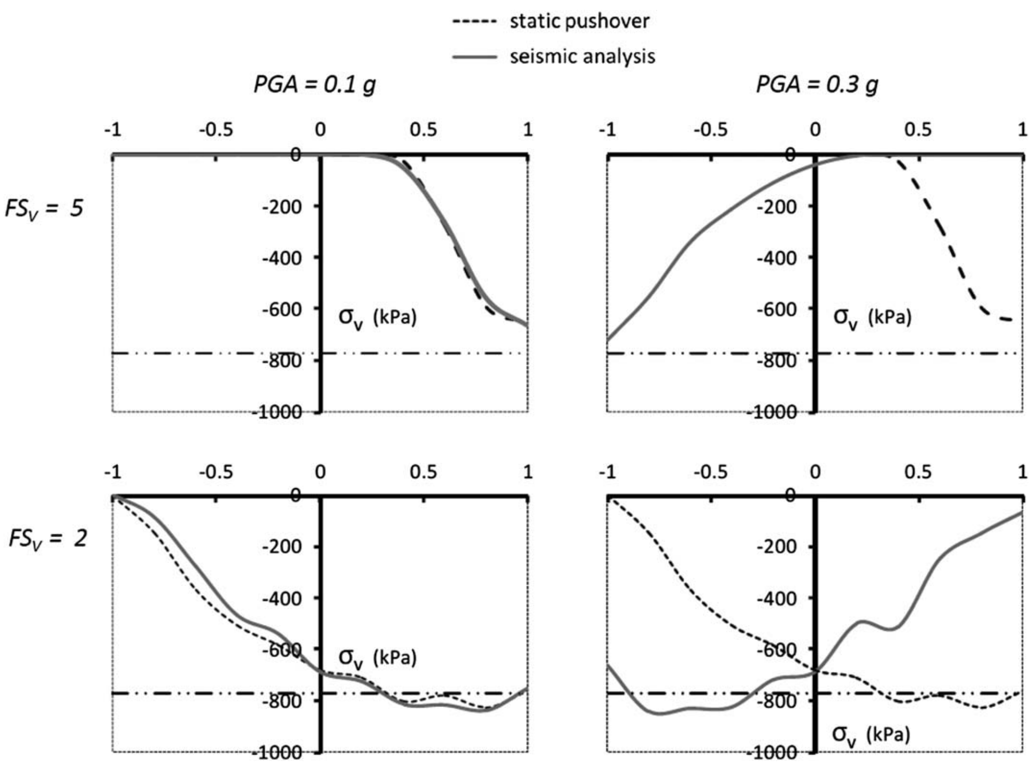

Figure 16. Distribution of soil-footing contact stresses under ultimate static and seismic loading. Their similarity is evident. The horizontal dotted line indicates Prandtl's $(\pi + 2)S_u$ value.

Comparison between the distribution of the vertical soil-footing contact stresses in the static and the dynamic analyses when the overturning moment reaches its maximum for each analysis are shown in Figure 16. Also indicated for comparison is the ultimate pressure $[(\pi + 2)\, S_u]$ of Prandlt's classical plasticity solution. The Prandlt solution seems to be the upper limit for the stresses below the footing even under (asymmetric) moment loading.

The two other accelerograms (Kalamata and Lefkada) were examined for their different frequency content and different detailed characteristics. Their effects are compared to those of Takatori in Figures 17 and 18. The three Tables in Figure 17 show in black which of the combinations of FS_V and PGA lead to collapse of the structure out of the 72 cases examined. Figure 18 compares the time histories of acceleration, rotation, and effective contact area ratio for the case $FS_V = 2$, PGA = 0.20 g. Clearly, for the same PGA value, the Takatori motion is more detrimental than the other two motions, which is predictable in view of its fatal long-period and long-duration pulses. The above conclusion is supported by:

- The larger number of overturned oscillators (43 out of 72) as compared with Kalamata's (8 out of 72) and Lefkada's (12 out of 72);
- The largest magnitude of both the rotation and uplifting of the footing (smallest λ ratio for substantial duration).

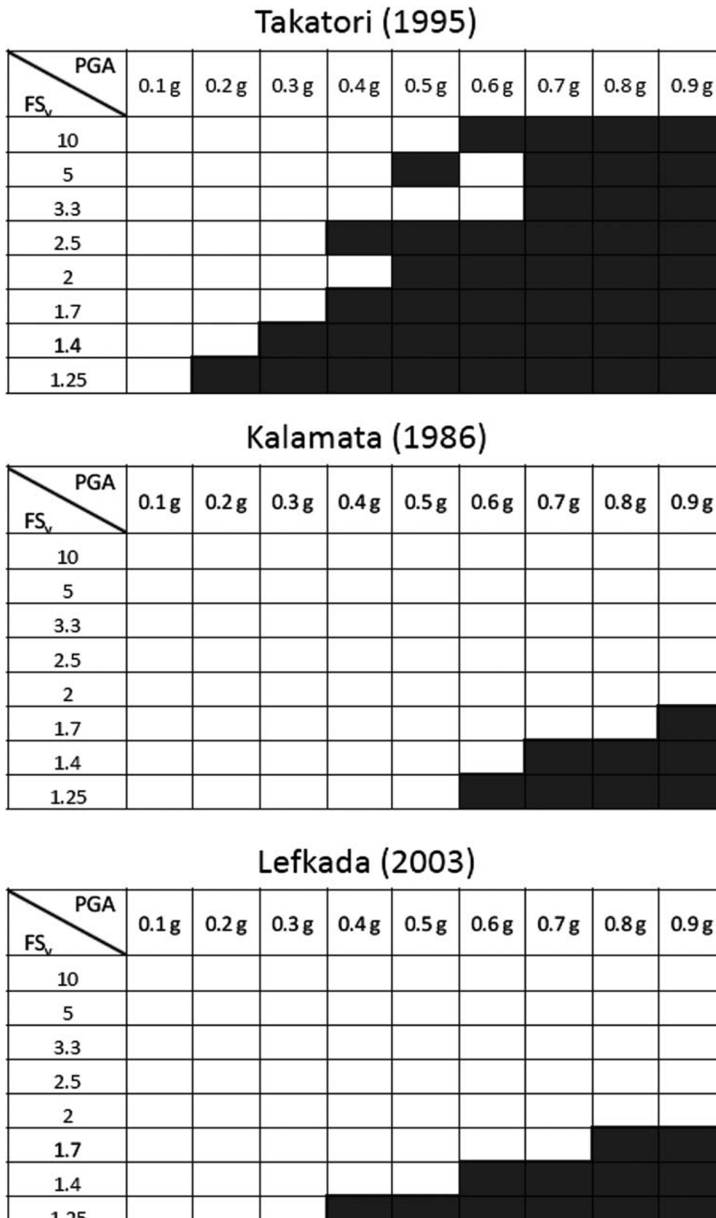

Figure 17. Collapse versus noncollapse cases for the three studied excitations scaled to PGA values ranging from 0.1 g to 0.9 g.

Moreover, note that the dominant period of oscillation depends appreciably on the frequency content of the input motion. This is attributed to the fact that this period depends strongly on how extensively uplifting takes place, which, among other parameters, is a function of the dominant frequencies of excitation. Thus the Takatori—and to a lesser degree the

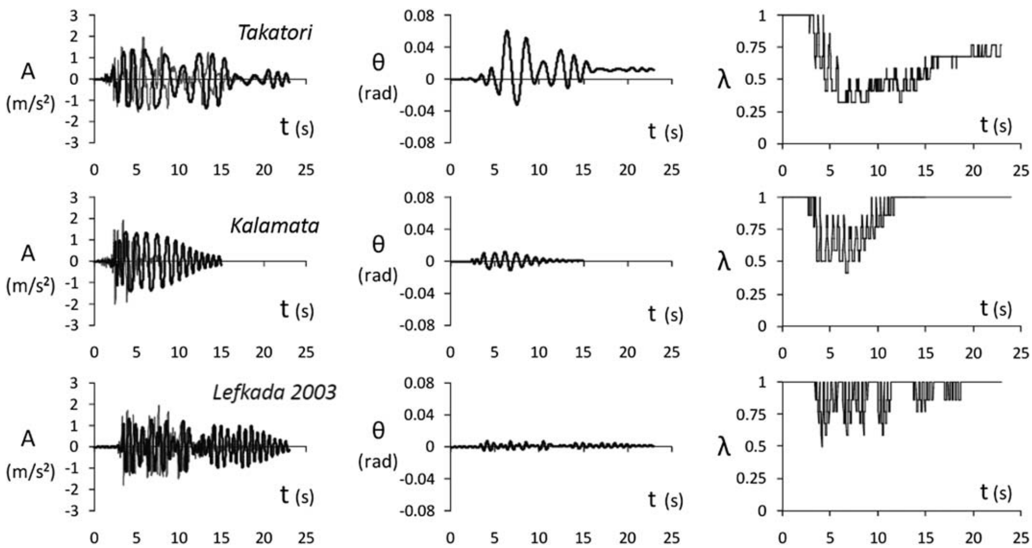

Figure 18. Comparisons of time histories of acceleration at mass, rotation of foundation, and ratio of soil-footing contact width to total width for the three studied excitations, sealed to 0.20 g.

Kalamata—scaled motions, with relatively strong unidirectional pulses, produce large rotation of the oscillator, and thereby significant uplifting (min $\lambda \approx 0.25$ and 0.50, respectively). On the other hand, the Lefkada motion has many almost symmetrical cycles without strong unidirectional pulses. This leads mostly to accumulation of settlement rather than rotation and uplifting. But despite the fact that the Kalamata motion produces significantly larger rotation, paradoxically, it is the Lefkada motion that is more "dangerous," as it can be inferred from the number of overturned oscillators (12 from Lefkada, 8 from Kalamata). This is attributed to the idiosyncrasies of the two accelerograms. Kalamata had one or two significant pulses and thus produces a few large irreversible rotations, but in the majority of the examined cases these are not critical. On the other hand, during the Lefkada motion (which had a low FS_V and high PGA), both settlement and rotation accumulate during its many cycles. As soil compliance increases, the unavoidably asymmetrical character of a real accelerogram becomes more apparent, resulting in the aforementioned asymmetric behavior of the system, the accumulation of rotation in one direction, and, eventually, collapse by overturning. Similar phenomena have been shown to occur with sliding and rocking systems on rigid base (Gazetas et al 2009, Makris and Roussos 2000, Gerolymos et al 2005).

IMPORTANT PARAMETERS NOT INVESTIGATED IN THE PAPER

Of the numerous problem parameters only two were studied here in some detail: the static factor of safety (FS_V) and the intensity and frequency content of the excitation. Detailed analysis of the significance of the following parameters could not possibly fit in the space of a single paper:

- The slenderness ratio h/b
- The absolute size of the system

- The flexibility of the superstructure (measured through its fixed-base period)
- The shape and embedment of the foundation
- The stiffness and strength of the soil

To an extent, changing these parameters from the values adopted in the paper may modify some of the conclusions of this work.

CONCLUSIONS

A relatively tall structure in comparison with the width of its foundation (slenderness ratio $h/b = 5$) founded on a saturated stiff clay ($S_u = 150$ kPa, $G_{max} = 105$ MPa) was numerically subjected to monotonic, cyclic, and seismic lateral loading. The vertical static factor of safety (FS_V) against bearing capacity failure was found to be a crucial parameter controlling the nature and amplitude of the response. Its effect was investigated parametrically for three seismic records of different frequency characteristics up- and down-scaled to PGA values ranging from 0.10 g to 0.60 g. The most important conclusions are as follows:

1. At such a high slenderness ratio, rocking is the dominant mode of oscillation. With high enough amplitudes of rotation the foundation undergoes uplifting from the supporting soil and generates alternating eccentric bearing capacity failure mechanisms under each compressed side of the footing. The prevalence of uplifting versus bearing capacity mechanisms is mainly controlled by FS_V, and secondarily by the intensity and frequency characteristics of the shaking. High values of FS_V (lightly loaded foundations) undergo mainly alternating uplifting; very low values of FS_V (heavily loaded foundations) mobilize the soil failure mechanisms.
2. The effect of gravity is to magnify the amplitude of rotation through the so-called P–delta effect. The moment-rotation diagram exhibits a descending branch and the occurrence of collapse is largely controlled by such an effect. This would be of practical significance for structures such as tall bridge piers, airport control towers, elevated water tanks, etc. (see some such applications in Gazetas 2001).
3. During cyclic and seismic excitation of a heavily loaded foundation ($FS_V < 3$), despite uplifting under the two edges, its center experiences an accumulating settlement. This behavior is of the same form as that experienced with foundations on dry sand, observed in many shake table experiments. By contrast, a lightly loaded foundation ($FS_V > 5$) experiences significant alternating uplifting, which leads to an insignificant (if any) additional settlement of the center of the foundation. This is different from the experimental observations on sand, in which development of volumetric strains under repeated (compaction-like) loading lead to accumulation of appreciable settlement. Such strains are not possible with the undrained conditions of our analysis.

ACKNOWLEDGEMENTS

The financial support to the project “DARE” has been provided by the European Research Council (ERC), through the Program “Ideas: Support of Frontier Research,” under contract number ERC–2008–AdG228254–DARE. We are thankful for this support. Andriani Panagiotidou expresses her gratitude for a scholarship from the Alexander Onassis Foundation.

REFERENCES

Allotey, N., and El Naggar, M. H., 2008. An investigation into the Winkler modeling of the cyclic response of rigid footings, *Soil Dynamics and Earthquake Engineering* **28**, 44–57.

Allotey, N., and El Naggar, M. H., 2003. Analytical moment-rotation curves for rigid foundations based on a Winkler model, *Soil Dynamics and Earthquake Engineering* **23**, 367–381.

Anastasopoulos, I., Gazetas, G., Loli, M., Apostolou, M., and Gerolymos, N., 2010. Soil failure can be used for seismic protection of structures, *Bulletin of Earthquake Engineering* **8**, 309–326.

Anastasopoulos, I., Georgarakos, T., Drosos, V., Giannakos, S., and Gazetas, G., 2009. Towards a reversal of seismic capacity design: Part B, Shaking-table testing of bridge pier-foundation system, in *Proceedings of the 3rd Greece-Japan Workshop on Seismic Design, Observation, and Retrofit of Foundations*, National Technical University of Greece, Santorini, 407–419.

Apostolou, M., Gazetas, G., and Garini, E., 2007. Seismic response of slender rigid structures with foundation uplifting, *Soil Dynamics and Earthquake Engineering* **27**, 642–654.

Apostolou, M., and Gazetas, G., 2005. Rocking of foundations under strong shaking: Mobilisation of bearing capacity and displacement demands, *1st Greece-Japan Workshop on Seismic Design, Observation, Retrofit of Foundations*, 11–12 October, 2005, Athens, Greece.

Bartlett, P. E., 1976. *Foundation Rocking on a Clay Soil*, ME thesis, Report No. 154, School of Engineering, University of Auckland, New Zealand.

Borja, R. I., Wu, W. H., and Smith, H. A., 1993. Nonlinear response of vertically oscillating rigid foundations, *Journal of Geotechnical Engineering* **119**, 893–911.

Borja, R. I., Wu, W. H., Amies, A. P., and Smith, H. A., 1994. Nonlinear lateral, rocking, and torsional vibrations of rigid foundations, *Journal of Geotechnical Engineering* **120**, 491–513.

Chatzigogos, C. T., Pecker, A., and Salençon, J., 2009. Macroelement modeling of shallow foundations, *Soil Dynamics and Earthquake Engineering* **29**, 765–781.

Chen, X. C., and Lai, Y. M., 2003. Seismic response of bridge piers on elastic-plastic Winkler foundation allowed to uplift, *Journal of Sound Vibration* **266**, 957–965.

Chopra, A. K., and Yim, C. S., 1984. Earthquake response of structures with partial uplift on Winkler foundation, *Earthquake Engineering and Structural Dynamics* **12**, 263–281.

Cremer, C., Pecker, A., and Davenne, L., 2002. Modeling of nonlinear dynamic behaviour of a shallow strip foundation with macro-element, *Journal of Earthquake Engineering* **6**, 175–211.

Dassault Systèmes, 2001. *ABAQUS 6.1 Standard User's Manual*, Providence, RI.

Dobry, R., and Gazetas, G., 1986. Dynamic response of arbitrarily–shaped foundations, *Journal of Geotechnical Engineering* **112**, 109–135.

Drosos, V., Georgarakos, T., Loli, M., Zarzouras, O., Anastasopoulos, I., and Gazetas, G., 2012. Soil-foundation-structure interaction with mobilization of bearing capacity: An experimental study on sand, *Journal of Geotechnical and Geoenvironmental Engineering, doi: 10.1061/(ASCE)GT.1943-5606.0000705.*

Faccioli, E., Paolucci, R., and Vanini, M., 1998. *3D Site Effects and Soil-Foundation Interaction in Earthquake and Vibration Risk Evaluation*, Final report of the European research project TRISEE, European Commission, Brussels, Belgium.

Faccioli, E., Paolucci, R., and Vivero, G., 2001. Investigation of seismic soil-footing interaction by large scale cyclic tests and analytical models, in *Proceedings of the 4th International Conference on Recent Advances in Geotechnical Earthquake Engineering and Soil Dynamics* (Prakash, S., ed.), CD-ROM, S. Prakash Foundation, San Diego, CA.

Fardis, M. N. (ed.), 2010. *Advances in Performance-Based Earthquake Engineering*, Springer, University of Patras, Greece, 485 pp.

Federal Emergency Management Agency (FEMA), 2000. *Prestandard and Commentary for the Seismic Rehabilitation of Buildings, FEMA-356*, Washington, D.C.

Figini, R., 2010. Nonlinear dynamic soil-structure interaction: Application to seismic analysis of structures on shallow foundations, Ph.D. thesis, Politecnico di Milano, Italy.

Gajan, S., Phalen, J.D., and Kutter, B. L., 2003. *Soil-Foundation-Structure Interaction: Shallow foundations, centrifuge data report for SSG03 test series, Report Nos. UCD/CGMDR-03/01 and 03/02*, Pacific Earthquake Engineering Research Center, University of California, Davis.

Gajan, S., Phalen, J. D., Kutter, B. L., Hutchinson, T. C., and Martin, G., 2005. Centrifuge modeling of load-deformation behavior of rocking shallow foundations, *Soil Dynamics and Earthquake Engineering* **25**, 773–783.

Gajan, S., and Kutter, B. L., 2008. Capacity, settlement, and energy dissipation of shallow footings subjected to rocking, *Journal of Geotechnical Geoenvironmental Engineering* **134**, 1129–1141.

Gajan, S., and Kutter, B. L., 2009a. Contact interface model for shallow foundations subjected to combined loading, *Journal of Geotechnical and Geoenvironmental Engineering* **135**, 407–419.

Gajan, S., and Kutter, B. L., 2009b. Effects of moment-to-shear ratio on combined cyclic load-displacement behavior of shallow foundations from centrifuge experiments, *Journal of Geotechnical and Geoenvironmental Engineering* **135**, 1044–1055.

Gazetas, G., 1987. Simple physical methods for foundation impedances, Chapter 2 in *Dynamics of Foundations and Buried Structures* (Benerjee, P. K., and Butterfield, R., eds), Elsevier Applied Science, Barking Essex, UK, 44–90.

Gazetas, G., 1991. Formulas and charts for impedances of surface and embedded foundation, *Journal of Geotechnical Engineering* **117**, 1363–1381.

Gazetas, G., 2001. SSI issues in two European projects and a recent earthquake, Paper S3 in *Proceedings of the 2nd U.S.-Japan Workshop on Soil-Structure Interaction* (Okawa, I., Iiba, M., and Celebi, M., eds.), Building Research Institute, Tsukuba, Japan.

Gazetas, G., and Apostolou, M., 2004. Nonlinear soil-structure interaction: Foundation uplifting and soil yielding, *3rd U.S.-Japan Workshop on Soil-Structure Interaction*, 29–30 March 2004, Menlo Park, CA.

Gazetas, G., and Apostolou, M., 2007. Shallow and deep foundations under fault rupture or strong seismic shaking, Chapter 9 in *Earthquake Geotechnical Engineering*, (Pitilakis, K., ed.), Springer Publishing, Dordrecht, The Netherlands, 185–215.

Gazetas, G., and Kavvadas, M., 2009. *Soil–Structure Interaction*, NTUA Publications, Athens, Greece.

Gazetas, G., Garini, E., and Anastasopoulos, I., 2009. Effect of near–fault ground shaking on sliding systems, *Journal of Geotechnical and Geoenvironmental Engineering* **135**, 1906–1921.

Georgiadis, M., and Butterfield, R., 1988. Displacements of footings on sands under eccentric and inclined loading, *Canadian Geotechnical Journal* **25**, 199–212.

Gerolymos, N., Apostolou, M., and Gazetas, G., 2005. Neural network analysis of overturning response under near-fault type excitation, *Earthquake Engineering and Engineering Vibration* **4**, 213–228.

Gerolymos, N., and Gazetas, G., 2006a. Development of Winkler model for static and dynamic response of caisson foundations with soil and interface nonlinearities, *Soil Dynamics and Earthquake Engineering* **26**, 363–376.

Gerolymos, N., and Gazetas, G., 2006b. Static and dynamic response of massive caisson foundations with soil and interface nonlinearities: Validation and results, *Soil Dynamics and Earthquake Engineering* **26**, 377–394.

Gottardi, G., Houlsby, G. T., and Butterfield, R., 1995. The displacement of a model rigid surface footing on dense sand under general planar loading, *Soils and Foundations* **35**, 71–82.

Harden, C. W., Hutchinson, T. C., Kutter, B. L., and Martin, G., 2005. *Numerical modelling of the nonlinear cyclic response of shallow foundation*, PEER Report 2005/04, Pacific Earthquake Engineering Research Center, Berkeley, CA.

Harden, C. W., Hutchinson, T. C., and Moore, M., 2006. Investigation into the effects of foundation uplift on simplified seismic design procedures, *Earthquake Spectra* **22**, 663–692.

Harden, C. W., and Hutchinson, T. C., 2009. Beam on nonlinear Winkler foundation modeling of shallow rocking–dominated footings, *Earthquake Spectra* **25**, 277–300.

Houlsby, G. T., Cassidy, M. J., and Einav, I., 2005. A generalized Winkler model for the behavior of shallow foundation, *Geotechnique* **55**, 449–460.

Housner, G. W., 1963. The behavior of inverted pendulum structures during earthquakes, *Bulletin of the Seismological Society of America* **53**, 403–417.

Huckelbridge, A. A., and Clough, R., 1978. Seismic response of uplifting building frame, *Journal of Structural Engineering* **104**, 1211–1229.

Ishibashi, I., and Zhang, X., 1993. Unified dynamic shear moduli and damping ratios of sand and clay, *Soils and Foundations* **33**, 112–191.

Ishiyama, Y., 1982. Motions of rigid bodies and criteria for overturning by earthquake excitations, *Earthquake Engineering Structural Dynamics* **10**, 635–650.

Kausel, E., 1974. *Forced Vibrations of Circular Foundations on Layered Media, Research Report R74-11*, Department of Civil Engineering, Massachusetts Institute of Technology, Cambridge, MA.

Kawashima, K., Nagai, T., and Sakellaraki, D., 2007. Rocking seismic isolation of bridges supported by spread foundations, in *Proceedings of 2nd Japan-Greece Workshop on Seismic Design, Observation, and Retrofit of Foundations*, Japanese Society of Civil Engineers, Tokyo, 254–265.

Kirkpatrick, P., 1927. Seismic measurements by the overthrow of columns, *Bulletin of the Seismological Society of America* **17**, 95–109.

Koh, A. S., Spanos, P., and Roesset, J. M., 1986. Harmonic rocking of rigid block on flexible foundation, *Journal of Engineering Mechanics* **112**, 1165–1180.

Kutter, B. L., Martin, G., Hutchinson, T. C., Harden, C., Gajan, S., and Phalen, J. D., 2006. *Workshop on modeling of nonlinear cyclic load-deformation behavior of shallow foundations*, PEER *Report* 2005/14, Pacific Earthquake Engineering Research Center, University of California, Berkeley, CA.

Luco, J. E., and Westman, R. A., 1971. Dynamic response of circular footings, *Journal of the Engineering Mechanics Division* **97**, 1381–1395.

Makris, N., and Roussos, Y., 2000. Rocking response of rigid blocks under near source ground motions, *Géotechnique* **50**, 243–262.

Martin, G. R., and Lam, I. P., 2000. Earthquake resistant design of foundations: Retrofit of existing foundations, *Geoengineering 2000 Conference (GeoEng2000)*, 19–24 November 2000, Melbourne, Australia.

Meek, J., 1975. Effect of foundation tipping on dynamic response, *Journal of Structural Division* **101**, 1297–1311.

Mergos, P. E., and Kawashima, K., 2005. Rocking isolation of a typical bridge pier on spread foundation, *Journal of Earthquake Engineering* **9**, 395–414.

Nakaki, D. K., and Hart, G. C., 1987. Uplifting response of structures subjected to earthquake motions, in *U.S.-Japan Coordinated Program for Masonry Building Research, Report No 2.1-3* (Ewing, Kariotis, Englekirk, and Hart, eds.).

Negro, P., Paolucci, R., Pedrett, S., and Faccioli, E., 2000. Large-scale soil-structure interaction experiments on sand under cyclic loading, Paper No. 1191, *12th World Conference on Earthquake Engineering*, 30 January–4 February 2000, Auckland, New Zealand.

Nova, R., and Montrasio, L., 1991. Settlement of shallow foundations on sand, *Géotechnique* **41**, 243–256.

Panagiotidou, A. I., 2010. *2D and 3D inelastic seismic response analysis of foundation with uplifting and P- Δ effects*, thesis, National Technical University, Athens, Greece.

Paolucci, R., 1997. Simplified evaluation of earthquake induced permanent displacement of shallow foundations, *Journal of Earthquake Engineering* **1**, 563–579.

Paolucci, R., and Pecker, A., 1997. Seismic bearing capacity of shallow strip foundations on dry soils, *Soils and Foundations* **37**, 95–105

Paulay, T., and Priestley, M. J. N., 1992. *Seismic Design of Reinforced Concrete and Masonry Buildings*, John Wiley & Sons, New York, NY.

Pecker, A., 1998. Capacity design principles for shallow foundations in seismic areas, keynote lecture, in *11th European Conference Earthquake Engineering* (Bisch, P., Labbe, P., and Pecker, A., eds.) A. A. Balkema, Rotterdam, The Netherlands, 303–315.

Priestley, M. J. N., 1993. Myths and fallacies in earthquake Engineering——Conflicts between design and Reality, *Bulletin, New Zealand Society for Earthquake Engineering* **26**, 329–341.

Priestley, M. J. N., Seible, F., and Calvi, G. M., 1996. *Seismic Design and Retrofit of Bridges*, John Wiley & Sons, New York, NY.

Priestley, M. J. N., 2003. Myths and fallacies in earthquake engineering, revisited, *Ninth Mallet-Milne Lecture*, Rose School, IUSS Press, Instituto Universitario di Studi Superiori, Pavia, Italy.

Roesset, J. M., 1980. Stiffness and damping coefficients of foundations, in *Dynamic Response of Foundations: Analytical Aspects* (O'Neil, M. W., and Dobry, R., eds.), American Society of Civil Engineers, Reston, VA, 1–30.

Rosebrook, K. R., and Kutter, B. L., 2001. *Soil-Foundations-Structure Interaction: Shallow foundations, Centrifuge data report*, Report Nos. UCD/CGMDR-01/09, 01/10, and 01/11, University of California, Davis, CA.

Salençon, J., and Pecker, A., 1995. Ultimate bearing capacity of shallow foundations under inclined and eccentric loads. Part II: Purely cohesive soil without tensile strength, *European Journal of Mechanics, A:Solids* **14**, 377–396.

Shi, B., Anooshehpoor, A., Zeng, Y., and Brune, J., 1996. Rocking and overturning of precariously balanced rocks by earthquake, *Bulletin of the Seismological Society of America* **86**, 1364–1371.

Shirato, M., Kouno, T., Nakatani, S., and Paolucci, R., 2007. Large-scale model tests of shallow foundations subjected to earthquake loads, in *Proceedings of the 2nd Japan-Greece Workshop on Seismic Design, Observation, and Retrofit of Foundations*, Japanese Society of Civil Engineers, Tokyo, Japan, 275–299.

Shirato, M., Kuono, T., Asai, R., Fukui, J., and Paolucci, R., 2008. Large scale experiments on nonlinear behavior of shallow foundations subjected to strong earthquakes, *Soils and Foundations* **48**, 673–692.

Taylor, P. W., and Williams, B. C., 1979. Foundations for capacity designed structures, *Bulletin of the New Zealand National Society for Earthquake Engineering* **12**, 101–113.

Vetetsos, A. S., and Wei, Y. T., 1971. Lateral and rocking vibration of footings, *Journal of the Soil Mechanics and Foundation Division* **97**, 1227–1248.

Villaverde, R., 2007. Methods to assess the seismic collapse capacity of buildings structures: State of the art, *Journal of Structural Engineering* **133**, 57–66.

Williamson, E. B., 2003. Evaluation of damage and P-Δ effects for systems under earthquake excitation, *Journal of Structural Engineering* **129**, 1036–1046.

Wolf, J. P., 1988. *Soil–Structure Interaction Analysis in Time-Domain*, Prentice–Hall, Englewood Cliffs, NJ.

(Received 10 February 2011; accepted 26 November 2011)